Pergamon

Int. J. Heat Mass Transfer Vol. 37, Suppl. 1, pp. 107–111, 1994
Elsevier Science Ltd

0017–9310/94 $6.00 + 0.00

0017–9310(93)E0078–U

Natural convection heat transfer in overlapping discrete plate arrays

P. BALASUNDAR and V. M. K. SASTRI†

Department of Mechanical Engineering, Indian Institute of Technology, Madras 600 036, India

Abstract—A numerical solution of the boundary layer equations was obtained using a finite difference formulation for natural convection in an array of vertical overlapping discrete plate segments. The results obtained are presented along with a comparison with the results for a continuous plate array. It was found that the overlapping arrays can enhance the heat transfer rate by as much as 80–90% for fixed values of the wall-to-ambient temperature difference and heat transfer area. The attainment of heat transfer enhancement by the use of discrete plates is possible only in certain ranges of the modified Rayleigh number.

INTRODUCTION

COOLING of electronic components by air, which is also the ultimate heat sink, is quite common in the electronics industry. Cooling by natural air convection is most preferable as it is highly reliable and avoids additional power consumption for forcing the air for cooling.

The developments in the electronic industry with increasingly higher integration of circuits lead to smaller semi-conducting devices with higher volumetric heat flux. Figure 1 shows the relationship between driving temperature difference and surface heat flux. Augmentation in natural convection is necessary to enhance the surface heat flux removal for a given driving temperature.

Aung *et al.* [1, 2] studied laminar free convection in an asymmetrically heated vertical parallel plate array and obtained the results for both uniform wall temperature and wall heat flux conditions. Carpenter *et al.* [3] investigated the combined radiation and free convection in a developing laminar flow between two parallel plates with asymmetric heating. The only prior analytical work on discrete plate segment array in natural convection is by Sparrow and Prakash [4, 5]. They considered an array of discrete plates in staggered and in-line arrangements, and a parallel plate array. They compared the heat transfer results for the three arrangements and identified the regime of enhancement.

The enhancement technique investigated in the present work involves the use of an array of staggered overlapping plates replacing an array of parallel plates. The objective is to obtain basic heat transfer data and to identify the regime of enhancement relative to the parallel plate array.

Numerical solutions of the coupled conservation equations for mass, momentum and energy are obtained for both arrangements for a fixed overlapping length. The Prandtl number is taken as 0.7 for air. The parameters are the modified Rayleigh number based on channel width and the number of plates in a channel, N.

The solution of the discrete plate array depends on both the parameters while the solution of the parallel plate array depends only on the modified Rayleigh number.

FORMULATION OF THE PROBLEM

Consider two parallel vertical plates separated by a distance $2S$, each of height H, and maintained at temperature T_w as shown in Fig. 2(a). Each of the parallel plates can be assumed to be made up of N plate segments of equal length L, so that the height of the plate $H = NL$.

When alternate plate segments are displaced horizontally by a distance S from the plane of each plate as shown in Fig. 2(b), a staggered arrangement results. Further, when the displaced plates are moved downward for a fixed overlap, it would result in a staggered overlapping arrangement as in Fig. 2(c). When such transformation is done in an array of vertical continuous parallel plates with interplate spacing of $2S$, it would result in a staggered overlapping plate segment array with interplate spacing of S. Figure 2(d) shows a staggered overlapping array.

The overlapping discrete plate array is considered to be very large in the z direction. Hence the fluid flow and heat transfer are two-dimensional. The velocity and temperature vary along the x and y coordinates only. Each channel, as in Fig. 2(d), is defined by two adjacent columns of plates and is a representative of the entire array. The lateral extremities are covered by vertical walls. These walls avoid any pressure com-

†Current address: Department of Mechanical Engineering, University of Delaware, Newark, DE 19716, U.S.A.

NOMENCLATURE

D_h	hydraulic diameter
Gr	Grashof number, $g\beta(T_w - T_\infty)D_h^3/v^2$
g	acceleration due to gravity
H	height of array (Fig. 2)
$\hat{H}$	dimensionless height, $(H/D_h)/Gr$
k	thermal conductivity
L	plate segment length (Fig. 2)
$\hat{L}$	dimensionless plate length, $(L/D_h)/Gr$
N	number of plates in a channel
P'	dimensionless difference pressure, $p(D_h^3/\rho v^2 Gr^2)$
P	pressure within array at x
P_∞	pressure in ambient at x
p'	difference pressure, $p - p_\infty$
Q	non-dimensional heat loss per unit breadth in a channel
Ra	Rayleigh number, $Gr \times Pr$
S	transverse interplate spacing (Fig. 2)
T	temperature
ΔT	temperature difference, $T_w - T_\infty$
U	dimensionless velocity, $(uD_h/v)Gr$
V	dimensionless velocity, vD_h/v
u, v	velocity components
X	dimensionless coordinate, $(x/D_h)/Gr$
Y	dimensionless coordinate, Y/D_h
x, y	coordinates (Fig. 2).

Greek symbols

β	thermal expansion coefficient
θ	dimensionless temperature, $(T - T_\infty)/(T_w - T_\infty)$
ν	kinematic viscosity
ρ	density.

Subscripts

d	discrete plate segment channel
p	parallel plate channel
∞	ambient external to the array

munication with the ambient, and it is assumed that bounding walls do not cause any thermal or hydrodynamic perturbation.

For the analysis, a subset of staggered overlapping array as shown in Fig. 2(e) is considered. The wall is considered to be isothermal at temperature T_w, which is higher then ambient temperature T_∞. The pressure at the inlet of the channel is p_o^1, and the pressure in the ambient in the same plane is p_o. The dynamic pressure at the inlet due to the flow is $p_o - p_o^1$, but this difference is very small as the velocities or flow are small. Thus, the pressure at the inlet of the channel is over-specified as p_o at the inlet instead of p_o^1. Hence

$$p = p_o - \rho g X. \tag{1}$$

In the ambient,

$$p_\infty(X) = p_o \rho_\infty g X \tag{2}$$

and inside the channel,

$$P(X) = p_o - \rho_x g X. \tag{3}$$

The density ρ_x decreases with the height due to heating, hence $p(X)$ is less than the ambient pressure $p_\infty(X)$. The difference in pressure $p'(X)$ is negative, i.e. the pressure inside the channel is less than the ambient, and this causes the flow of air through the channel. The equilibrium of flow rate through the system results from a balance between pressure drop and buoyancy. For given height, H, and heat transfer surface, the hydraulic diameter D_h for parallel plate and discrete plate segment array is evaluated according to ref. [8], namely $D_h = 4S$.

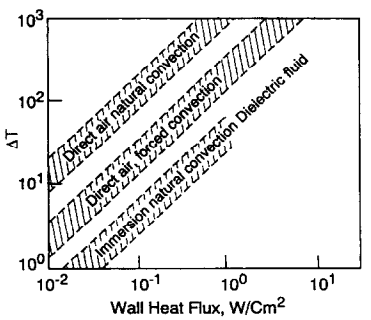

FIG. 1. Comparison of driving temperature in various modes of cooling.

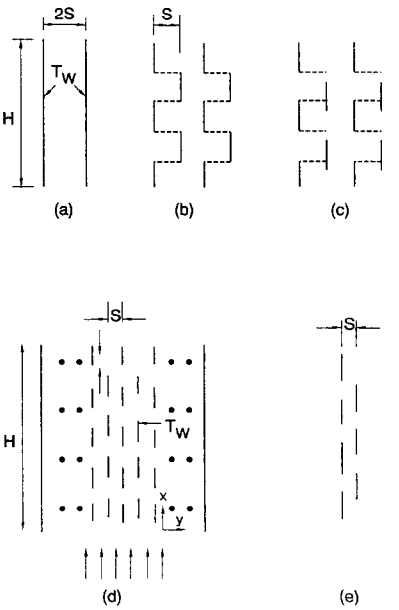

FIG. 2. The physical model.

The density–temperature relation $(\rho_\infty - \rho) = \beta\rho \times (T - T_\infty)$, equations (2) and (3) and the difference pressure are used to rewrite the buoyancy term in the momentum equation as

$$-\frac{\partial p}{\partial x} - \rho g = -\frac{\partial p'}{\partial x} + g(\rho_\infty - \rho) \tag{4}$$

$$= -\frac{\partial p'}{\partial x} + g\beta\rho(T - T_\infty). \tag{5}$$

The difference in pressure is very close to zero at the exit plane, owing to the external imposed pressure. However, for convenience, the $p'(x)$ at exit is underspecified as zero. The unknown variables u, v, p and T and the coordinates x and y are transformed suitably to dimensionless variables U, V, P, θ, X and Y. The governing equations become

$$\frac{\partial U}{\partial X} + \frac{\partial V}{\partial Y} = 0 \tag{6}$$

$$U\frac{\partial U}{\partial X} + V\frac{\partial U}{\partial Y} = -\frac{\partial P'}{\partial X} + \theta + \frac{\partial^2 U}{\partial Y^2} \tag{7}$$

$$U\frac{\partial \theta}{\partial X} + V\frac{\partial \theta}{\partial Y} = \frac{\partial^2 \theta}{\partial Y^2}. \tag{8}$$

The boundary conditions are $U = V = 0$ and $\theta = 1$ on the solid surface, and $\partial V/\partial Y = \partial\theta/\partial Y = V = 0$ on the symmetry lines. The additional conditions are

$$P' = 0 \quad \text{at} \quad X = 0$$
$$P' = 0 \quad \text{at} \quad X = \hat{H}.$$

For a given $\hat{H}$, it is difficult to find the corresponding inlet velocity U_0. However, if U_0 is assumed, then it is easy to find the corresponding $\hat{H}$ using the information about the pressure. In the finite difference method used to obtain the solution, a variable grid generated by a cosine function is used along the interplate spacing to minimize the computational time and loss of accuracy. For n grid points excluding the boundary to determine U, V and θ at all grid points and the pressure at that level $3n+1$ equations are needed. Since the governing equations yield only $3n$ equations, an extra equation is required to obtain a unique solution. This is obtained from the condition that the steady state mass throughout is constant along the height,

$$M = \int_0^{D_h} U\,dy. \tag{9}$$

The overall heat transfer in a channel over a height X is obtained as

$$Q(X) = \int_0^{D_h} U\theta\,dy. \tag{10}$$

SOLUTION PROCEDURE

The energy, x-momentum and steady state equations are solved for U, θ and P'. Then the continuity equation is used to obtain the value of V. The marching procedure is started at $X = 0$, where $p' = 0$. As one proceeds upwards, P' becomes negative, and after attaining a minimum value, increases to a positive pressure. The calculation is stopped as soon as the pressure becomes non-negative, hence, closely satisfying the condition $P' = U$ at $X = 0$ and at $X = \hat{H}$. The overall heat transfer is calculated up to that level. The number of grid points taken along the interplate spacing is 49, and about 200–3500 steps along the height are required.

PARALLEL PLATE ARRAY

The geometry for a parallel plate array is shown in Fig. 2(a). The solution for the parallel plate array is obtained in the same way using the same formulation with the corresponding boundary conditions, $U = V = 0$ and $\theta = 1$ on the solid surface. It should be noted that the value of D_h remains the same for both configurations. The discrete plate array is a transformation from a single plate. The value of Q obtained using equation (10) for the parallel plate array is divided by 2, to obtain the value of Q based on same area as the discrete plate array.

RESULTS AND DISCUSSION

The heat transfer data are obtained for discrete plate and parallel plate arrangements. Since

$$\hat{H} = \frac{H}{D_h Gr} = \frac{H\,Pr}{D_h Ra}, \text{ also } \hat{H} = N\hat{L}, \quad \text{and}$$

$$(D_h/H)Ra = Pr/N\hat{L}. \tag{11}$$

For a fixed value of N and for various plate lengths L $(D_h/H)Ra$ values are calculated. This can be repeated for various N values.

The heat transfer data obtained from the computer solution using equation (10), as discussed in the preceding section, are represented in Fig. 3. The values

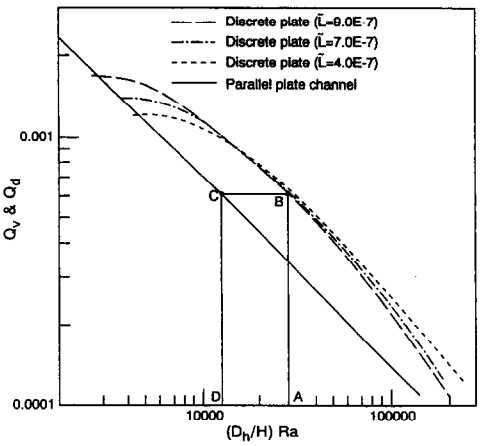

FIG. 3. Overall heat transfer results for discrete plate and parallel plate array.

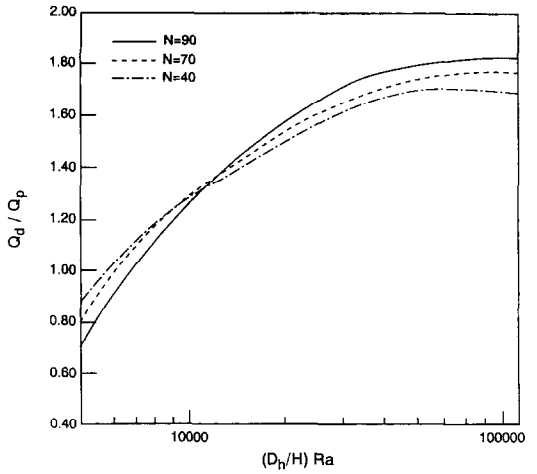

FIG. 4. Comparison of heat transfer performance of discrete plate and parallel plate arrays.

of Q_d and Q_p can be obtained for height $\hat{H}$, read from this graph. The ratio Q_d/Q_p is then plotted as a function of $(D_h/H)Ra$ with the number of plates in the channel N as a parameter (Fig. 4).

As seen in the Fig. 4, there is substantial enhancement for a large range of the abscissa variable; the enhancement is greater with larger number of plates and higher values of $(D_h/H)Ra$. An increase in $(D_h/H)Ra$ with fixed D_h means a smaller value of H. Hence enhancement is greater when H is small. Further, above $(D_h/H)Ra$ of about 2300, the enhancement is greater with a larger number of plates (i.e. higher N value at fixed $(D_h/H)Ra$) and with larger transverse spacing (i.e. larger $(D_h/H)Ra$ at fixed H).

The inefficiency of the discrete plate segment array at larger heights could be attributed to the reduced mass flow rate. As seen in Fig. 5, U_0, which is the indication of mass flow rate, is lower for discrete plate array then for parallel plate array at larger height. This is due to the additional pressure drop incurred in restarting of the boundary layer over each plate segment.

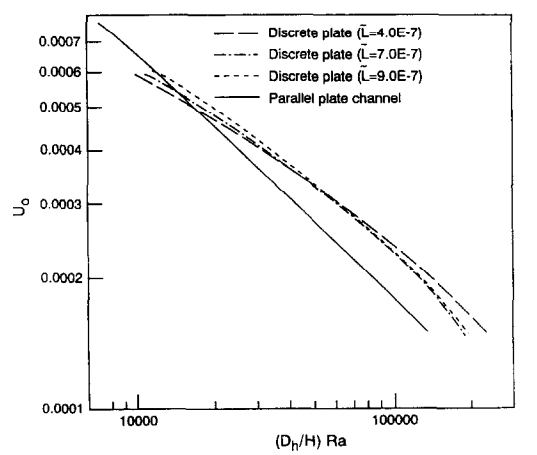

FIG. 5. Comparison of inlet velocity results for discrete plate and parallel plate arrays.

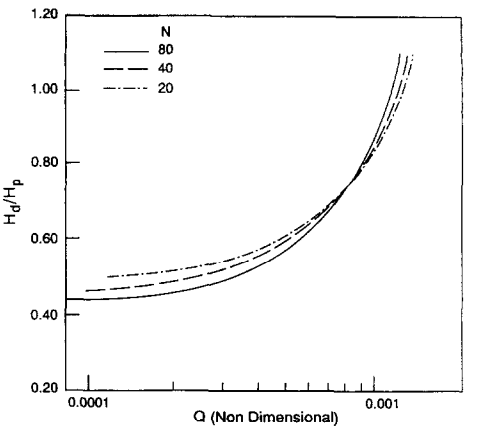

FIG. 6. Comparison of array height for discrete and parallel plate arrays at fixed Q.

Array height comparisons

The array height for fixed heat dissipation, Q, of the discrete plate segment array is compared with that of the parallel plate array. The graph (Fig. 6) is obtained for various N values. To this end, $(D_h/H)Ra$ is obtained for several values of the plate length $\hat{L}$ using equation (9). From Fig. 3 the Q_d is obtained for each corresponding value of $(D_h/H)Ra$. Further, for the same heat loss Q_d, $(D_h/H)Ra$ for a parallel plate array is also obtained. A typical example of the procedure is shown in Fig. 3 (ABCD).

The ratio H_d/H_p is plotted against Q. In Fig. 6, it can be seen that for smaller values of Q, H_d/H_p is less then one and remains constant and thus at larger heat loss range, the overlapping discrete plate segment array becomes ineffective.

Pressure distribution along height

The distribution of dimensionless difference, pressure P', is shown in Fig. 7, the ordinate being the ratio of the local value of p' to the minimum value of p' for the case under consideration. A typical case considered for plotting is with a minimum value of

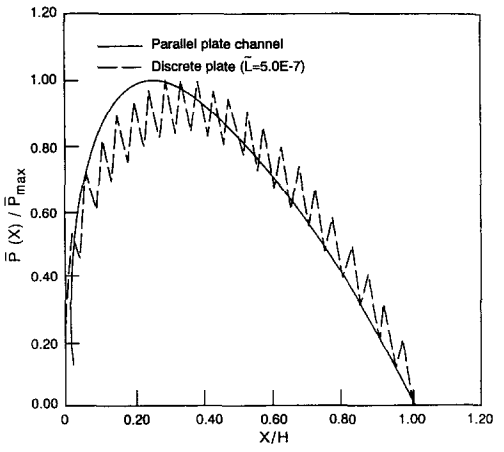

FIG. 7. Axial distribution of inner ambient pressure difference along height H.

$p' = -2.5 \times 10^{-7}$ for the parallel plate array and discrete plate arrays with $N = 21$. The difference pressure decreases with X from the inlet plane and attains the minimum value and then increases to zero.

Conclusions

It is concluded that heat transfer enhancement is significant for the discrete plate array compared to the parallel plate arrangement provided the $(D_h/H)Ra$ value is more than a certain value. It is further noted that the critical value becomes smaller for larger values of $\hat{L}$.

REFERENCES

1. W. Aung, L. S. Fletcher and V. Sernas, Developing laminar free convection between vertical flat plates with asymmetric heating, *Int. J. Heat Mass Transfer* **15,** 2293 (1972).
2. W. Aung, Fully developed laminar free convection between heated vertical plates heated asymmetrically, *Int. J. Heat Mass Transfer* **15,** 1577 (1972).
3. J. R. Carpenter, D. G. Briggs and V. Sernas, Combined radiation and developing laminar free convection between vertical flat plate with asymmetric heating, *J. Heat Transfer* **98,** 94 (1976).
4. E. M. Sparrow and C. Prakash, Enhancement of natural convection heat transfer by a staggered array of discrete vertical plates, *J. Heat Transfer* **102,** 215 (1980).
5. C. Prakash and E. M. Sparrow, Natural convection heat transfer performance evaluation for discrete (in-line or staggered) and continuous-plate arrays, *Numer. Heat Transfer* **3,** 89 (1980).
6. J. R. Bodoia and J. F. Osterle, The development of free convection between heated vertical plates, *J. Heat Transfer* **84,** 40 (1962).
7. G. P. Peterson and A. Ortega, Thermal control of electronic equipment and devices, *Adv. Heat Transfer* **20,** 181 (1990).
8. W. M. Kays and A. L. London, *Compact Heat Exchangers* (2nd Edn). McGraw-Hill, New York (1964).